Development 134, 2459-2468 (2007) doi:10.1242/dev.001958

Cxcl12/Cxcr4 chemokine signaling is required for placode assembly and sensory axon pathfinding in the zebrafish olfactory system

Nobuhiko Miyasaka[1,2,*], Holger Knaut[3] and Yoshihiro Yoshihara[1,2]

Positioning neurons in the right places and wiring axons to the appropriate targets are essential events for establishment of neural circuits. In the zebrafish olfactory system, precursors of olfactory sensory neurons (OSNs) assemble into a compact cluster to form the olfactory placode. Subsequently, OSNs differentiate and extend their axons to the presumptive olfactory bulb with high precision. In this study, we aim to elucidate the molecular mechanism underlying these two developmental processes. *cxcr4b*, encoding a chemokine receptor, is expressed in the migrating olfactory placodal precursors, and *cxcl12a* (*SDF-1a*), encoding a ligand for Cxcr4b, is expressed in the abutting anterior neural plate. The expression of *cxcr4b* persists in the olfactory placode at the initial phase of OSN axon pathfinding. At this time, *cxcl12a* is expressed along the placode-telencephalon border and at the anterior tip of the telencephalon, prefiguring the route and target of OSN axons, respectively. Interfering with Cxcl12a/Cxcr4b signaling perturbs the assembly of the olfactory placode, resulting in the appearance of ventrally displaced olfactory neurons. Moreover, OSN axons frequently fail to exit the olfactory placode and accumulate near the placode-telencephalon border in the absence of Cxcr4b-mediated signaling. These data indicate that chemokine signaling contributes to both the olfactory placode assembly and the OSN axon pathfinding in zebrafish.

KEY WORDS: Stromal cell-derived factor-1 (SDF-1), GPCR, Cell migration, Axon guidance, Pioneer axons, Zebrafish

INTRODUCTION

Cell positioning and axon pathfinding are developmental processes crucial for the formation of neural circuits and the proper functioning of the nervous system. During early development, neuronal precursors migrate from their birthplace to their final destination along characteristic routes. Upon reaching their destination, the neuronal precursors differentiate and extend axons to the specific targets. Both processes require navigation through a complex environment. Many molecules that have been discovered initially for their functions in axon guidance turn out to also play important roles in cell migration, and vice versa (de Castro, 2003; Guan and Rao, 2003), suggesting that these two developmental processes use common guidance mechanisms, at least in part.

The olfactory system is an excellent model for studying both cell migration and axon guidance. Olfactory sensory neurons (OSNs) develop within the olfactory placode, a thickened ectoderm that later gives rise to the olfactory epithelium (OE). Subsequently, OSNs extend axons toward the developing olfactory bulb (OB) with exquisite precision. In zebrafish, a previous fate map study has revealed that a large cellular field located along the lateral edge of the anterior neural plate converges through cell movements to form the olfactory placode (Whitlock and Westerfield, 2000). However, the factors responsible for directing the assembly of the olfactory placode have not yet been identified.

[1]Laboratory for Neurobiology of Synapse, RIKEN Brain Science Institute, 2-1 Hirosawa, Wako-shi, Saitama 351-0198, Japan. [2]Core Research for Evolutional Science and Technology, Japan Science and Technology Agency, Osaka 560-0082, Japan. [3]Department of Molecular and Cellular Biology, Harvard University, 16 Divinity Avenue, Cambridge, MA 02138, USA.

*Author for correspondence (e-mail: miyasaka@brain.riken.jp)

Accepted 12 April 2007

Chemokines are small, secreted proteins that were originally identified as molecules regulating leukocyte trafficking in the immune system. Recently, it has become clear that chemokines and their receptors play prominent roles, not only in the immune response, but also in various cellular events during development of the nervous system (Tran and Miller, 2003). In particular, Cxcl12 (also known as SDF-1, stromal cell-derived factor-1) influences the guidance of both migrating neurons (Bagri et al., 2002; Zhu et al., 2002; Stumm et al., 2003; Belmadani et al., 2005; Knaut et al., 2005; Borrell and Marin, 2006) and growing axons (Xiang et al., 2002; Chalasani et al., 2003; Li et al., 2005; Lieberam et al., 2005) through its receptor Cxcr4. As the olfactory placode is one of the regions where Cxcr4 is expressed during embryogenesis (Chong et al., 2001; Tissir et al., 2004; Schwarting et al., 2006), it is conceivable that Cxcl12/Cxcr4 signaling may play a role in olfactory development. Here, we provide genetic evidence demonstrating that Cxcl12/Cxcr4 signaling mediates the assembly of olfactory placodal precursors into a compact cluster to form the olfactory placode in zebrafish. Furthermore, the loss of Cxcl12/Cxcr4 signaling results in impaired pathfinding of pioneer olfactory axons and failure of OSN axons to project to the OB. Our results indicate that chemokine signaling plays a dual role in controlling cell positioning and subsequent axon pathfinding during early development of the primary olfactory system in zebrafish.

MATERIALS AND METHODS

Fish maintenance

Zebrafish, *Danio rerio*, were maintained and embryos were collected essentially as described (Westerfield, 1995). Embryos were staged according to hours postfertilization (hpf) at 28.5°C and morphological criteria (Kimmel et al., 1995). Collected embryos were maintained in 1/3 Ringer's solution (39 mM NaCl, 0.97 mM KCl, 1.8 mM $CaCl_2$, 1.7 mM HEPES, pH 7.2) supplemented with 100 units/ml penicillin and 100 μg/ml streptomycin. In some cases, 0.002% phenylthiourea (PTU) was added after 12 hpf to prevent pigmentation. We confirmed that PTU treatment at a dose of 0.002% does

not affect olfactory placode assembly and OSN axon projection, although the treated embryos show a slight delay of hatching, as observed in previous work (Elsalini and Rohr, 2003).

Fish lines

A transgenic line, Tg(OMP^{2k}:gap-YFP)^{rw032a} (abbreviated as omp:yfp), in which membrane-tethered YFP is expressed under the control of the olfactory marker protein (OMP) promoter, were used to visualize olfactory neurons, including unipolar pioneer neurons and ciliated OSNs (Miyasaka et al., 2005; Sato et al., 2005). *odysseus* (*ody*) homozygous adults were crossed with heterozygous adults to obtain ~50% *ody*/*ody* embryos and ~50% *ody*/+ embryos for synchronized development. *ody*/*ody* embryos were identified by the impaired migration of germ cells (Doitsidou et al., 2002; Knaut et al., 2003) and neuromasts (David et al., 2002), as assessed by immunofluorescence staining for Vasa (a marker for germ cells) and PCAM (a marker for neuromasts and OSNs; also known as Ncam3 – ZFIN), respectively. In some cases, *ody* mutant embryos were genotyped by PCR amplification of DNA fragments containing the *ody* mutant locus, followed by direct sequencing of the PCR products. Primers used are as follows: ody-f, 5′-TGGAGTTTGGCTTCCAGCGAC-3′; ody-r, 5′-CAGCATAGTCA-AAGCGTCCAC-3′. A transgenic line, hsp:cxcl12a (previously called *heatshock*-SDF-1a) (Knaut et al., 2005) was used for ubiquitous heat-induced misexpression of Cxcl12a.

Whole-mount in situ hybridization

cDNA fragments for probes against *cxcl12a*, *cxcl12b*, *cxcr4a*, *cxcr4b*, *cxcr7a* and *cxcr7b* were amplified by PCR from cDNA libraries of zebrafish embryos or adult heads. Zebrafish *cxcr7* orthologs to the human and mouse *Cxcr7* gene were identified by TBLASTN searches using the sixth draft zebrafish genome assembly (Zv6: Sanger Center). The sequences used as probes against *cxcr7a* and *cxcr7b* were deposited in GenBank with the accession numbers EF467374 and EF467375, respectively. Digoxigenin (DIG)-labeled cRNA probes were generated by in vitro transcription from their cDNA clones. Whole-mount in situ hybridization was performed as previously described (Miyasaka et al., 2005).

Immunohistochemistry

Whole-mount immunohistochemistry was carried out as previously described (Miyasaka et al., 2005), with the following modifications. Embryos were fixed overnight at 4°C in 4% paraformaldehyde in PBS and permeabilized in acetone for 7 minutes at –20°C.

Antibodies used are as follows: rabbit polyclonal anti-GFP antibody (1:1000, a kind gift from Dr N. Tamamaki, Kumamoto University, Kumamoto, Japan); rat monoclonal anti-GFP antibody (1:1000, Nacalai Tesque); mouse monoclonal zns-2 antibody (1:20, supernatant, Developmental Studies Hybridoma Bank); rabbit polyclonal anti-PCAM antibody (rabbit IgG; 0.4 μg/ml) (Mizuno et al., 2001; Miyasaka et al., 2005); rabbit polyclonal anti-Vasa antibody (1:2000) (Knaut et al., 2000); rabbit polyclonal anti-DsRed antibody (1:300, Clontech); Cy3-conjugated donkey anti-mouse IgG antibody (1:300, Jackson ImmunoResearch); Cy3-conjugated goat anti-rabbit IgG antibody (1:300, Jackson ImmunoResearch); Alexa 488-conjugated goat anti-rabbit IgG antibody (1:300, Molecular Probes); Alexa 488-conjugated goat anti-rat IgG antibody (1:300, Molecular Probes); peroxidase-conjugated goat anti-rabbit IgG Fab antibody fragment [Histofine Simple Stain Max PO(R), Nichirei Bioscience].

Morpholino injection

Antisense morpholino oligonucleotides (MOs: Gene Tools, LLC) were dissolved at a concentration of 4 ng/nl in 1× Danieau buffer [58 mM NaCl, 0.7 mM KCl, 0.4 mM $MgSO_4$, 0.6 mM $Ca(NO_3)_2$, 5 mM HEPES, pH 7.6] containing 0.1% Phenol Red, and injected into one-cell stage embryos carrying the *omp:yfp* transgene at a volume of 1 nl with an air pressure microinjector (FemtoJet, Eppendorf). The volume of MO solution to be injected was calibrated by measuring the diameter of a droplet at the tip of glass needle in the air. MO sequences are as follows: *cxcr4b* MO, 5′-AAA TGA TGC TAT CGT AAA ATT CCA T-3′ (Doitsidou et al., 2002); *cxcl12a* MO, 5′-ACT TTG AGA TCC ATG TTT GCA GTG-3′ (Li et al., 2005); *cxcl12b* MO, 5′-CGC TAC TAC TTT GCT ATC CAT GCC A-3′ (Knaut et al., 2003).

Cxcl12a misexpression

For ubiquitous misexpression, *hsp:cxcl12a/+* fish were crossed with *omp:yfp/+* fish. Embryos obtained from such a cross were heat shocked at either 12 hpf or 19 hpf for 1 hour in a 37°C water bath, raised at 28.5°C, and imaged at 26-29 hpf and 3.5 days postfertilization (dpf) using a confocal laser-scanning microscope (Olympus FV500). To identify hsp:cxcl12a transgenic embryos, genomic DNAs were extracted from the embryos after image acquisition, and genotyped by PCR using the following primers: 5′-CAT GTG GAC TGC CTA TGT TCA TC-3′; 5′-ATC AGA GCG ACT ACT ACG ATC AC-3′.

For mosaic misexpression, *omp:yfp/+* embryos were injected at the one- to two-cell stage with a 50 μg/ml solution of phsp:mDsRed or phsp:cxcl12a-mDsRed DNA, and heat shocked at 12 hpf and again at 19 hpf. The second heat-shock treatment was given to facilitate identification of cells expressing mDsRed or Cxcl12a-mDsRed. The embryos were fixed at 24 hpf and analyzed by immunohistochemistry using anti-GFP and anti-DsRed antibodies. The DNA constructs were prepared as follows. To generate phsp:mDsRed, *EGFP* cDNA of the pHSP70/4-EGFP (Halloran et al., 2000) was removed by *Age*I and *Not*I digestion and replaced with *DsRed-Monomer* cDNA from the pDsRed-Monomer (Clontech). To generate phsp:cxcl12a-mDsRed, the stop codon of *cxcl12a* was removed by PCR and the *cxcl12a* gene was inserted between the *Sal*I and *Age*I sites of the phsp:mDsRed so that the *DsRed-Monomer* was in frame with the last codon of the *cxcl12a* gene.

Time-lapse imaging

Embryos younger than 2 dpf were anesthetized in 0.016% tricaine and mounted in 1.5% low-melting point agarose. Embryos older than 2.5 dpf were anesthetized, inserted into a silicone tube (1 mm inner diameter, 2.5 mm outer diameter, 5 mm length) to allow the embryos to stand, and mounted anterior side down on a glass-bottomed petri dish with a small amount of 1/3 Ringer's solution. The embryos were imaged at each time point using a confocal microscope. The embryos were removed from the agarose or silicon tube and kept at 28.5°C between the time points for observations.

RESULTS

Spatiotemporal expression patterns of *cxcl12a* and *cxcr4b* correlate with the olfactory placode formation and olfactory axon pathfinding

A previous study has shown that mRNA for Cxcr4b is prominently expressed in the olfactory placode at 24 hpf (Chong et al., 2001), suggesting that this receptor might play a role in the development of the olfactory system. To corroborate this possibility, we analyzed the spatiotemporal expression of *cxcr4b* in the head region in more detail. At 12 hpf, *cxcr4b* was expressed in a row of cells along the anterolateral edge of the neural plate (Fig. 1A) that corresponds to the presumptive olfactory placodal field (Whitlock and Westerfield, 2000). During the next few hours, *cxcr4b*-expressing cells increased in number and arranged at the edge of the developing anterior neural tube, forming bilateral bands along the anteroposterior axis (Fig. 1C,E). By 20 hpf, most of the *cxcr4b*-expressing cells had assembled into the olfactory placode (Fig. 1G,I). From 24 to 30 hpf, when the initial olfactory axons were extending toward the developing OB, *cxcr4b* expression in the olfactory placode was still evident (Fig. 1K,M,O), but cells adjacent to the apical surface, where mature OSNs reside, were devoid of *cxcr4b* expression (Fig. 1O). From 36 hpf onward, *cxcr4b* expression in the olfactory placode was greatly diminished, and only a few cells expressing *cxcr4b* remained in the basal part of the OE at 48 hpf (Fig. 1Q,S).

In the zebrafish genome, there are two genes (*cxcl12a* and *cxcl12b*) that encode potential ligands for Cxcr4b. Analyzing the expression patterns of the two Cxcr4b ligands, we found that only *cxcl12a* (right panels in Fig. 1), but not *cxcl12b* (see Fig. S1D-F in

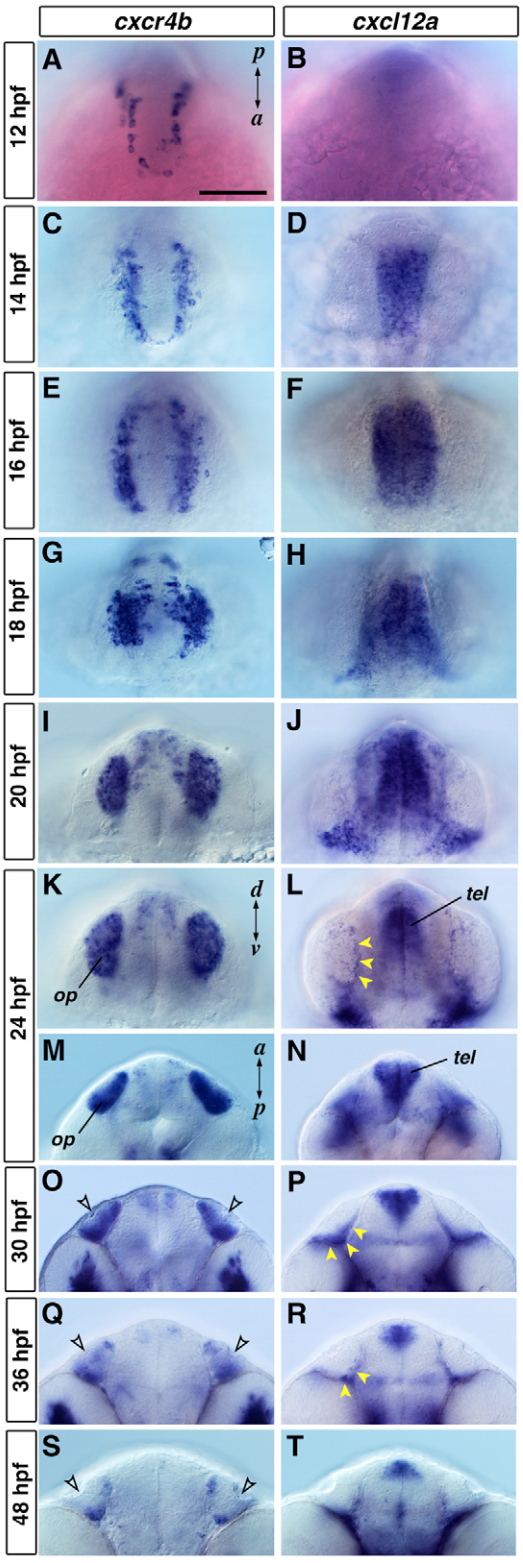

Fig. 1. Expression patterns of *cxcr4b* and *cxcl12a* during development of the olfactory placode in zebrafish. Whole-mount in situ hybridization analysis of *cxcr4b* (left panels) and *cxcl12a* (right panels) expression in the anterior head during the first 2 days of embryonic development. (**A-D**) Dorsal views with anterior to the bottom. (**E-H**) Frontodorsal views with anteroventral to the bottom. (**I-L**) Frontal views with ventral to the bottom. (**M-R**) Dorsal views with anterior to the top. (**S**,**T**) Ventral views with anterior to the top. From 12 to 16 hpf, *cxcr4b* is expressed bilaterally along the anterior-lateral edge of developing neural tube (A,C,E), whereas *cxcl12a* is expressed medially adjacent to the *cxcr4b*-expressing bilateral stripes (D,F). Progressive convergence of *cxcr4b*-expressing domains occurs between 16 and 20 hpf (E,G,I) to form the olfactory placodes. *cxcr4b* expression in the olfactory placode persists during initial phase of axon pathfinding (K,M,O,Q,S), although cells near the olfactory pit (arrowheads in O,Q,S) are devoid of *cxcr4b* expression. At the same period, *cxcl12a* expression is detected at the olfactory placode-telencephalon border (arrowheads in L,P,R), as well as in the anterior tip of telencephalon. Scale bar: 100 μm. *a*, anterior; *d*, dorsal; *op*, olfactory placode; *p*, posterior; *tel*, telencephalon; *v*, ventral.

the supplementary material), was present in close proximity to the *cxcr4b*-expressing olfactory placode. The developing anterior neural tube was located between the two *cxcr4b*-expressing stripes and started to express *cxcl12a* by 14 hpf (Fig. 1D). Over the next ten hours, the *cxcl12a* expression domain gradually became restricted to the anterior tip of the telencephalon (Fig. 1F,H,J,L) and the two *cxcr4b*-expressing stripes closely followed this refining *cxcl12a* expression and, by convergence movements, formed the two olfactory placodes (Fig. 1E,G,I,K). At 24 to 36 hpf, in addition to the telencephalic expression, *cxcl12a* was expressed by cells residing at the basal margin of the olfactory placode, on the border between the placode and the telencephalon where olfactory axons cross to enter the telencephalon (Fig. 1L,P,R). At 48 hpf, the expression of *cxcl12a* in the telencephalon was less intense but still visible, while the expression in the margin of the OE was barely detectable (Fig. 1T). Thus, the expression of *cxcl12a* in close proximity to *cxcr4b*-expressing cells that will form the olfactory placodes is consistent with the idea that chemokine signaling might play a role in olfactory placode assembly and OSN axon pathfinding.

Cxcl12a/Cxcr4b signaling is required for the olfactory placode assembly

To assess the role of Cxcr4b-mediated chemokine signaling in the formation of the olfactory placode, we analyzed *odysseus* (*ody*) mutants, in which a nonsense mutation in the third intracellular loop leads to a truncation of Cxcr4b and probably creates a loss of Cxcr4b function (Knaut et al., 2003). *ody*/*ody* or *ody*/+ embryos were examined for *cxcr4b* expression during the period of olfactory placode formation. At 12 and 14 hpf, the arrangement of cells expressing *cxcr4b* in *ody*/*ody* embryos was indistinguishable from that in *ody*/+ embryos (Fig. 2A,B,F,G). At 16 hpf, some *cxcr4b*-expressing cells in *ody*/*ody* embryos were not arranged along the lateral edge of the developing anterior neural tube and dispersed laterally or anteromedially (Fig. 2H). At 18 hpf, a substantial number of *cxcr4b*-expressing cells were mispositioned ventromedially (Fig. 2I). At 20 hpf, when the olfactory placode had formed, the ventromedially displaced cells were still detectable at ectopic positions, although reduced in number (Fig. 2J). Total number of *cxcr4b*-expressing cells in the anterior head region of *ody*/*ody* embryos did not differ from that of *ody*/+ embryos during the period of olfactory placode assembly [*ody*/*ody* versus *ody*/+, 51±4 versus 51±2 cells/side (16 hpf), 85±2 versus 83±2 (18 hpf), 98±5 versus 103±3 (20 hpf), n=6 for each, mean±s.e.m.], suggesting that the loss of Cxcr4b-mediated signaling causes mispositioning of olfactory placodal precursors without affecting their proliferation.

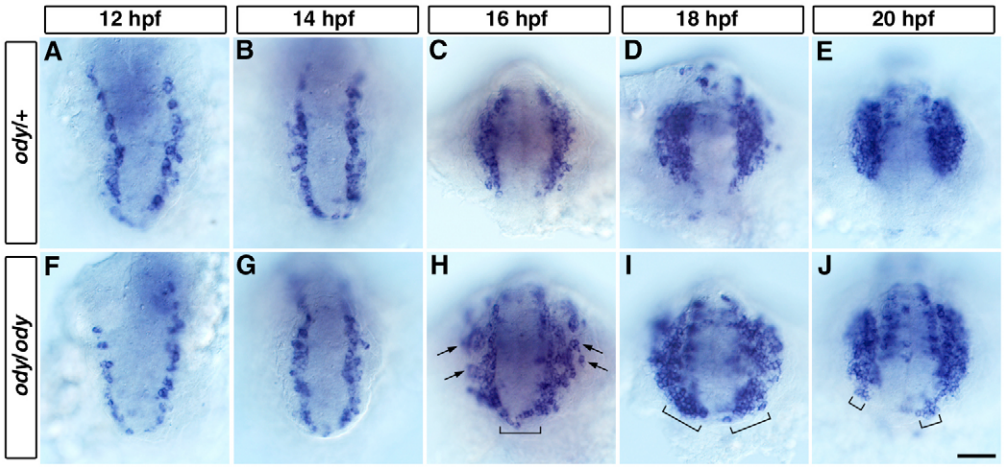

Fig. 2. Assembly of *cxcr4b*-expressing cells into the olfactory placode is perturbed in *ody*/*ody* embryos. Zebrafish *ody*/*ody* and *ody*/+ embryos were hybridized with cRNA probe against *cxcr4b*. (**A**,**B**,**F**,**G**) Dorsal views with anterior to the bottom. (**C**,**D**,**H**,**I**) Frontodorsal views with anteroventral to the bottom. (**E**,**J**) Frontal views with ventral to the bottom. At 12 and 14 hpf, the arrangement of *cxcr4b*-expressing cells in *ody*/*ody* embryos (F,G) is indistinguishable from that in *ody*/+ embryos (A,B). At 16 hpf, *cxcr4b*-expressing cells in *ody*/*ody* embryos disperse laterally (arrows in H) and anteroventrally (bracket in H) away from the lateral edge of developing neural tube. At 18 hpf, substantial numbers of *cxcr4b*-expressing cells are mispositioned ventrally (brackets in I). By 20 hpf, some *cxcr4b*-expressing cells (brackets in J) fail to join a cluster positioned at the correct site of the olfactory placode. Scale bar: 50 μm.

To examine whether the mispositioned cells in *ody*/*ody* embryos develop into olfactory neurons, we used the omp:yfp transgenic line in which membrane-tethered EYFP starts to be expressed at ~20 hpf in a subpopulation of olfactory neurons, including unipolar pioneer neurons and ciliated OSNs (Miyasaka et al., 2005; Sato et al., 2005). In *ody*/*ody* embryos carrying the *omp:yfp* transgene, YFP-positive cells were less tightly organized than those in wild-type embryos and often dispersed ventromedially from the normal position of the olfactory placode at 24 hpf (Fig. 3A-C). Similarly, reducing the expression level of Cxcr4b by MO-mediated knockdown frequently led to a mispositioning of YFP-positive cells at 24 hpf (Fig. 3D), mimicking the phenotype observed in *ody* mutants. The fact that mispositioned cells express YFP under the control of the *omp* promoter suggests that the specification of olfactory neurons is independent of Cxcr4b signaling. To trace the subsequent fate of these ectopically located olfactory neurons, we analyzed *ody* mutants until 3.5 dpf. The ectopically positioned YFP-positive olfactory neurons observed at 1 dpf were rapidly reduced in number during the second day of development, and they had completely disappeared by 3.5 dpf (Fig. 9E-H).

As Cxcl12a, a ligand for Cxcr4b, is expressed in the adjacent neural tube located medially to the *cxcr4b*-expressing olfactory placodal precursors, we asked whether Cxcl12a is also required for correct olfactory neuron positioning. To address this issue, we reduced the activity of Cxcl12a by MO injection and analyzed the position of YFP-positive olfactory neurons at 24 hpf. *cxcl12a* MO-injected embryos (morphants) frequently displayed ventromedially mispositioned olfactory neurons (Fig. 3E), as observed in *ody* mutants (Fig. 3B,C) and *cxcr4b* morphants (Fig. 3D). Consistent with the absence of expression in the vicinity of the developing olfactory system, reducing the activity of Cxcl12b, another ligand for Cxcr4b, did not perturb olfactory neuron positioning (Fig. 3F).

Due to phenotypic variability in embryos with compromised *cxcr4b*-mediated signaling (Fig. 3), we quantitated to what degree olfactory neurons are mispositioned at 24 hpf by measuring the distances from the midline to the medialmost and lateralmost cells (medial and lateral limits), and the distances from the ventral edge of the head to the ventralmost and dorsalmost cells (ventral and dorsal limits) (Fig. 4). In wild-type embryos, virtually no olfactory placode failed to assemble, although two out of 30 placodes showed a ventromedial displacement of a single olfactory neuron (Fig.

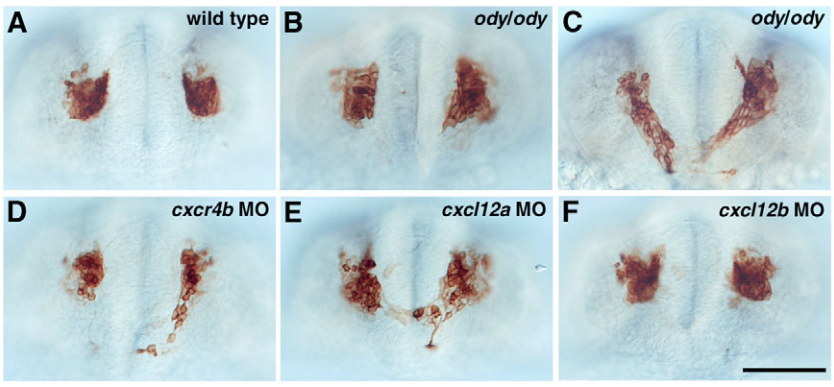

Fig. 3. Cxcl12*a*/Cxcr4b signaling is required for olfactory neuron positioning. Wild-type zebrafish embryos (**A**), *ody* mutants (**B**,**C**), *cxcr4b* MO-injected embryos (morphants) (**D**), *cxcl12a* morphants (**E**) and *cxcl12b* morphants (**F**), which all carry the *omp:yfp* transgene, were stained with anti-GFP antibody at 24 hpf to visualize olfactory neurons. All panels show frontal views with ventral to the bottom. Two representative *ody*/*ody* embryos with mild (B) and severe (C) defects in olfactory neuron positioning are shown. Scale bar: 100 μm.

DEVELOPMENT

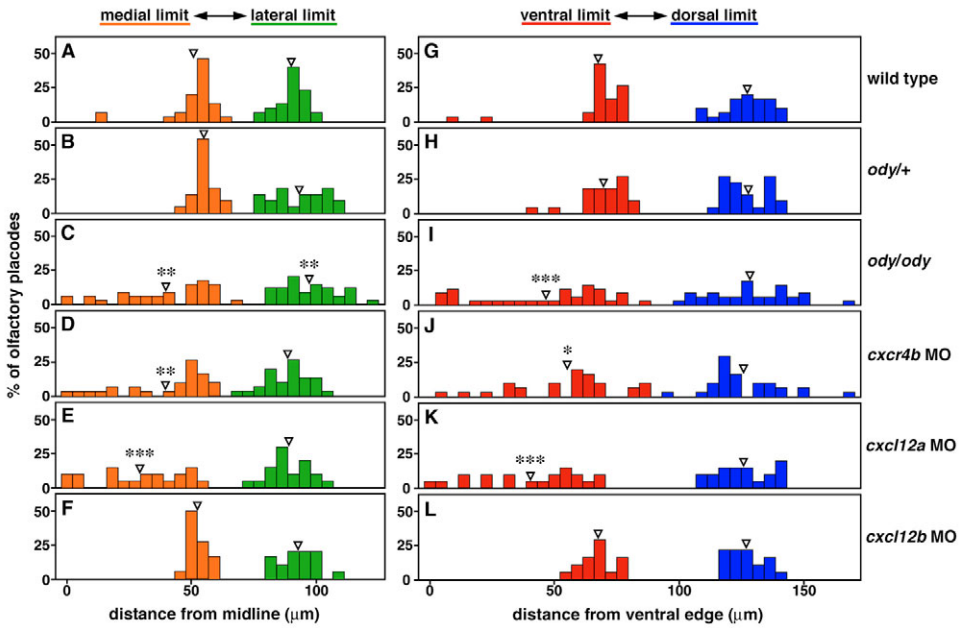

Fig. 4. Quantification of olfactory neuron mispositioning. (**A-L**) Distances from the midline to the medialmost and lateralmost cells (medial and lateral limits), and distances from the ventral edge of the head to the ventralmost and dorsalmost cells (ventral and dorsal limits) in individual olfactory placodes were measured from the images of 24 hpf zebrafish embryos stained with anti-GFP antibody (e.g. Fig. 3). Percentages of olfactory placodes that display indicated medial (orange), lateral (green), ventral (red) and dorsal (blue) limits are shown as bar graphs in wild-type embryos (A,G; *n*=30 placodes), *ody*/+ embryos (B,H; *n*=22), *ody*/*ody* embryos (C,I; *n*=34), *cxcr4b* morphants (D,J; *n*=30), *cxcl12a* morphants (E,K; *n*=20) and *cxcl12b* morphants (F,L; *n*=18). Arrowheads indicate the averaged distance of each limit. *, *P*<0.05; **, *P*<0.01; ***, *P*<0.001, compared with wild-type; *t*-test.

4A,G). In *ody*/+ embryos (Fig. 4B,H) and *cxcl12b* morphants (Fig. 4F,L), essentially no olfactory placode displayed mispositioning of olfactory neurons. By contrast, a large proportion of placodes in *ody*/*ody* embryos (Fig. 4C,I), *cxcr4b* morphants (Fig. 4D,J) and *cxcl12a* morphants (Fig. 4E,K) exhibited ventromedially displaced olfactory neurons; the averages of ventral limit (*ody*/*ody*, 47±4 μm, *n*=34; *cxcr4b* MO, 55±4 μm, *n*=30; *cxcl12a* MO, 40±5 μm, *n*=20; mean±s.e.m.) and medial limit (*ody*/*ody*, 40±3 μm, *n*=34; *cxcr4b* MO, 40±3 μm, *n*=30; *cxcl12a* MO, 29±4 μm, *n*=20) were significantly shifted ventrally and medially, respectively, when compared with wild-type placodes (ventral limit, 68±3 μm; medial limit, 51±2 μm; *n*=30). In *ody*/*ody* embryos, the average of lateral limit was slightly shifted laterally when compared with wild type (*ody*/*ody*, 97±2 μm, *n*=34; wild type, 90±1 μm, *n*=30), but neither *cxcr4b* nor *cxcl12a* morphants showed such a shift. Thus, ventromedial displacement of olfactory neurons is a common phenotype when reducing or removing Cxcl12a/Cxcr4b signaling. These results indicate that Cxcl12a signaling through Cxcr4b is required for assembly of the olfactory neuron precursors into a compact cluster.

The ventromedial mispositioning in *cxcl12a* morphants appeared more severe than that in either *ody*/*ody* embryos or *cxcr4b* morphants (Fig. 4C-E,I-K). This observation raises a possibility that olfactory neuron precursors may express a second receptor for Cxcl12a. To address this issue, we analyzed the expression of other Cxcl12a candidate receptors. We found that *cxcr4a*, the other *cxcr4* homolog, was not expressed in the developing olfactory placode (see Fig. S1G-I in the supplementary material). Recent studies in mammals have shown that Cxcl12 also binds to and signals through an alternate chemokine receptor, Cxcr7 (also known as Rdc1 and Cmkor1) (Balabanian et al., 2005; Burns et al., 2006). We searched the zebrafish genome database and identified two genes (*cxcr7a* and *cxcr7b*) equally homologous to the mammalian *cxcr7*. In situ hybridization analyses revealed that neither *cxcr7a* nor *cxcr7b* was expressed in the developing olfactory placode (see Fig. S1M-R in the supplementary material). These results indicate that Cxcr4b is the only known Cxcl12a receptor expressed in the olfactory neuron precursors, suggesting that olfactory neuron precursors can sense Cxcl12a only through Cxcr4b during placode assembly.

Misexpression of Cxcl12a perturbs the olfactory placode assembly

The Cxcl12a expression domain at the anterior neural tube becomes restricted to the anterior tip of the telencephalon simultaneously with the assembly of the olfactory placode (Fig. 1), suggesting that Cxcl12a might act as a directional cue to guide migration of olfactory placodal precursors. To test this possibility, we first sought to perturb the local source of Cxcl12a by raising the Cxcl12a levels throughout the embryo. We heat shocked hsp:cxcl12a;omp:yfp double-transgenic embryos before (12 hpf) and after (19 hpf) olfactory placode assembly, and analyzed the positioning of YFP-positive olfactory neurons at 26-29 hpf. Embryos in which Cxcl12a was heat induced at 12 hpf (six of 11 embryos) showed impaired assembly of olfactory neurons (Fig. 5B), which resembled the Cxcl12a/Cxcr4b morphant and *ody* mutant phenotypes (Fig. 3). Heat induction of Cxcl12a at 19 hpf (*n*=12) did not affect the placode assembly (Fig. 5C). Similarly, heat shocking omp:yfp single transgenic embryos did not cause any defects in olfactory neuron assembly (Fig. 5A). These results suggest that a spatially and temporally localized Cxcl12a source is crucial for correct positioning of olfactory neurons.

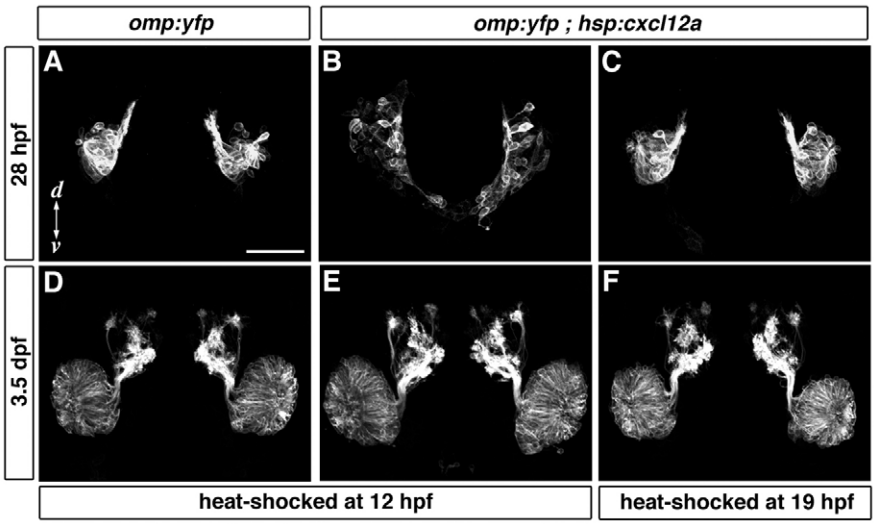

Fig. 5. Ubiquitous misexpression of Cxcl12a perturbs olfactory neuron assembly but does not affect projection of olfactory axons. *omp:yfp/+* and *omp:yfp/+;hsp:cxcl12a/+* zebrafish embryos were heat shocked at either 12 or 19 hpf. Using confocal microscope, positioning of olfactory neurons and subsequent projection of olfactory axons were viewed in the same individuals at 28 hpf (**A-C**) and 3.5 dpf (**D-F**), respectively. Composite images generated from a series of optical sections are shown. Heat induction of Cxcl12a at 12 hpf (B), but not 19 hpf (C), perturbs assembly of olfactory neurons. Heat shocking itself does not affect the positioning of olfactory neurons (A). None of the Cxcl12a heat-induced embryos display an impaired projection of olfactory axons at 3.5 dpf (D-E). All panels show frontal views. Scale bar: 100 μm. *d*, dorsal; *v*, ventral.

Next, to determine whether Cxcl12a attracts migrating olfactory neuron precursors, we analyzed the effects of localized Cxcl12a misexpression. We injected omp:yfp transgenic embryos with a DNA construct containing a monomeric DsRed (mDsRed)-tagged Cxcl12a under the control of *hsp70* promoter, creating ectopic sources of Cxcl12a after heat shock. In embryos that showed mosaic Cxcl12a-mDsRed expression in the anterior head, we frequently observed abnormal appearance of YFP-labeled olfactory neurons ventral to the correct position (n=14 of 16 embryos). In such cases, some olfactory neurons were found in close proximity to the ventral ectopic Cxcl12a sources (Fig. 6B-D). By contrast, we never found dorsally displaced olfactory neurons, despite the presence of ectopic sources in the dorsal region (open arrowheads in Fig. 6B). In control embryos with mosaic mDsRed expression in the anterior head (n=15), olfactory placode assembly was never perturbed (Fig. 6A). These results indicate that ectopically expressed Cxcl12a in the ventral region can compete with the endogenous Cxcl12a and recruit olfactory neurons ventrally.

OSN axon projection is impaired in the absence of Cxcl12a/Cxcr4b signaling

As *cxcr4b* expression persists in the olfactory placode at the initial phase of olfactory axon pathfinding, and *cxcl12a* is expressed along the route of olfactory axon outgrowth (Fig. 1), we investigated whether the loss of Cxcl12a/Cxcr4b signaling affects OSN axon projection to the OB. OSNs are composed of two major types of neurons, ciliated and microvillous OSNs, which express different types of odorant receptors and display distinct glomerular innervation in a mutually exclusive manner (Sato et al., 2005). Using the PCAM antibody, a marker that labels axons from both ciliated and microvillous OSNs (Miyasaka et al., 2005), we examined axon trajectories of OSNs in *ody* mutants at 3 dpf, when prototypic glomerular targeting by OSN axons has been established. In *ody* mutants, we frequently observed an impaired OSN axon projection (Fig. 7). Due to phenotypic variability, we divided *ody* mutants into three classes: 28% of the *ody* mutants (n=18 embryos) showed bilateral OSN axon projection defects (class 3); 28% showed projection defects only on one side (class 2); and 44% showed normal axon projection to the OB (class 1). In *ody* mutants with projection defects, OSN axons failed to exit the OE or occasionally stalled immediately after exiting the OE, accumulating near the OE-telencephalon border (Fig. 7C,D). Intriguingly, embryos with projection defects on one side showed no detectable proto-glomerular innervation defects on the contralateral side (Fig. 7C). OSN axon projection defects were also seen when a subpopulation of OSN axons were labeled by membrane-tethered YFP in *ody* mutants carrying the *omp:yfp* transgene (Fig. 9H). Reducing the

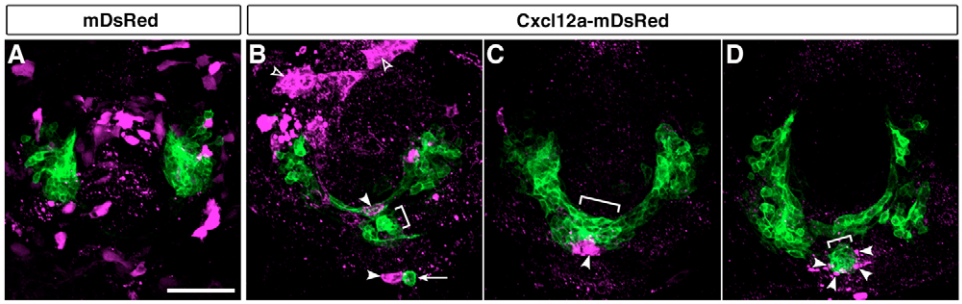

Fig. 6. Localized Cxcl12a misexpression displaces olfactory neurons ventrally. Confocal *z*-stacked images of zebrafish embryos labeled with anti-GFP (green) and anti-DsRed (magenta) antibodies. All panels show frontal views with dorsal to the top. (**A**) *omp:yfp/+* embryo injected with phsp:mDsRed. Mosaic expression of mDsRed (magenta) does not affect positioning of YFP-expressing olfactory neurons (green). (**B-D**) Three examples of *omp:yfp/+* embryos injected with phsp:cxcl12a-mDsRed. YFP-expressing olfactory neurons do not coalesce into a compact cluster. Some neurons (brackets and arrow) are found at positions close to the ventral ectopic sources of Cxcl12a-mDsRed (arrowheads). By contrast, no olfactory neurons are displaced to positions near the dorsal ectopic sources (open arrowheads). Scale bar: 100 μm.

DEVELOPMENT

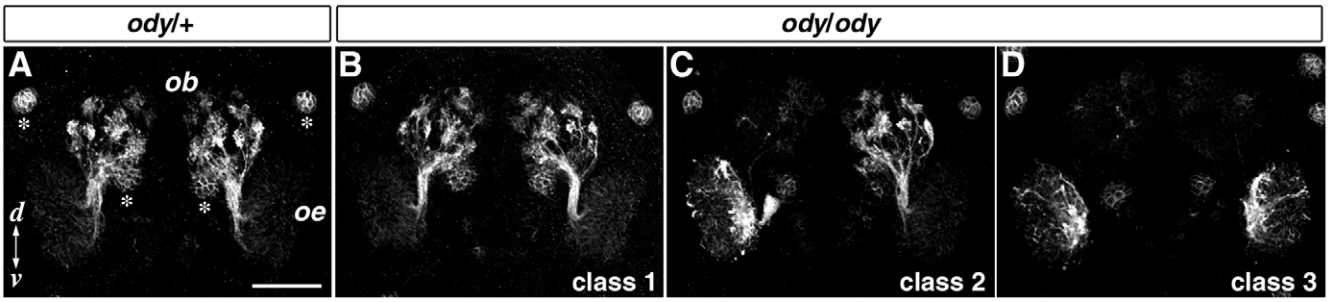

Fig. 7. Zebrafish *ody* mutant embryos show OSN axon projection defects. (**A-D**) Axon trajectories from both ciliated and microvillous OSNs are labeled at 3 dpf by whole-mount immunohistochemistry with anti-PCAM antibody, and are shown in frontal views as *z*-stacked images. *ody/ody* embryos are classified into three groups according to the severity of axon pathfinding defects (B-D): class 1 (8 of 18 embryos), a virtually wild-type projection pattern; class 2 (5 of 18), unilatetal projection defects; class 3 (5 of 18), bilateral projection defects. Projection patterns of all *ody/+* embryos (*n*=15) fall into class 1. Asterisks in A indicate neuromasts in the lateral line system. Scale bar: 100 μm. *d*, dorsal; *ob*, olfactory bulb; *oe*, olfactory epithelium; *v*, ventral.

activity of Cxcr4b by MO injections yielded similar defects in OSN axon projection, although the incidence of the defects was lower when compared with that of *ody* mutants (4 and 41% of OE, respectively; Table 1). Such a discrepancy in phenotypic incidence between mutants and morphants was not observed in the defects of the olfactory placode assembly (see Fig. 4). *cxcl12a* morphants also exhibited similar defects in OSN axon projection at a comparable incidence with *cxcr4b* morphants (3 and 4% of OE, respectively; Table 1), whereas *cxcl12b* morphants never displayed OSN axon projection defects (*n*=134 OE). The lower incidence of defects in *cxcl12a/cxcr4b* morphants than *ody* mutants that lack Cxcr4b function is probably explained by an incomplete removal of Cxcl12a/Cxcr4b signaling after MO injections. These results indicate that Cxcl12a/Cxcr4b signaling is important to allow OSN axons to exit the OE and to extend toward the OB, and suggest that the OSN axon projection would be ensured by less activity of Cxcl12a/Cxcr4b than that required for the olfactory placode assembly.

Pathfinding of pioneer olfactory axons is impaired in *odysseus* mutants

A previous study has demonstrated that the earliest axons growing to the presumptive OB originate from a transient population of neurons in the olfactory placode: the unipolar pioneer neurons.

Table 1. Summary of phenotypes caused by interfering with Cxcl12/Cxcr4 signaling

	Olfactory placode assembly*	Olfactory axon projection (% OE with no axon projection)
Wild type	Normal	Normal (0%, *n*=264)
ody/+	Normal	Normal (0%, *n*=162)
ody/ody	Disorganized	Impaired (41%, *n*=68)
cxcr4b MO	Disorganized	Impaired (3%, *n*=62)
cxcl12a MO	Disorganized	Impaired (4%, *n*=76)
cxcl12b MO	Normal	Normal (0%, *n*=134)
Ubiquitous Cxcl12a (HS at 12 hpf)	Disorganized	Normal†
Ubiquitous Cxcl12a (HS at 19 hpf)	Normal	Normal†

All embryos carry the *omp:yfp* transgene and the phenotypes are assessed by observing YFP-labeled cell bodies and axons at 1 dpf and 3 dpf, respectively.
*For details, see Fig. 4.
†Embryos obtained by crossing *hsp:cxcl12a/+* adults with wild-type adults exhibit normal axon projection after heat shock (HS) at either 12 hpf (*n*=113 embryos) or 19 hpf (*n*=145 embryos).

Ablation of these unipolar neurons perturbs pathfinding of axons from later developing OSNs (Whitlock and Westerfield, 1998), suggesting that the axons of unipolar neurons may provide a track for OSN axons to follow. Therefore, it is possible that Cxcr4b-mediated signaling helps axons of unipolar neurons to pioneer to the presumptive OB. To explore this possibility, we investigated the trajectory of pioneer axons of 1.5 dpf *ody* mutant embryos expressing YFP in both unipolar neurons and ciliated OSNs. Axons of unipolar neurons were identified by co-labeling with zns-2 antibody (Whitlock and Westerfield, 1998). We found that most of the YFP-positive axons emerging from the olfactory placode at 1.5 dpf were also immunoreactive for zns-2, and that projection of double-labeled pioneer axons were frequently impaired in *ody* mutant embryos (Fig. 8). The defects in pioneer axon projection from *ody* mutant olfactory placodes did not occur in an all-or-none manner, differently from PCAM-positive OSN axon projection at 3 dpf (see Fig. 7). In 19% of the *ody* mutant placodes, all pioneer axons failed to exit the placode and accumulated near the placode-telencephalon border (*n*=16 placodes; Fig. 8A-C); in 19% some pioneer axons reached the presumptive OB and the remaining axons failed to exit the placode (Fig. 8D-F), and in 62% most pioneer axons showed a normal projection to the presumptive OB (Fig. 8G-I). *ody/+* (see Fig. 9B) and wild-type (Fig. 8J-L) embryos never exhibited such pioneer axon projection defects.

To assess whether the variable projection patterns of pioneer axons from unipolar neurons are associated with projection patterns of following OSN axons, we carried out time-lapse observation of the YFP-expressing axons from both unipolar neurons and ciliated OSNs until 3.5 dpf. We found that about 44% of the *ody* mutant olfactory placodes (*n*=16) extended a smaller number of pioneer axons toward the presumptive OB (arrow in Fig. 9F) than did *ody/+* and wild-type olfactory placodes at 1.5 dpf. Whenever we observed the pioneer axons clearly not reaching the presumptive OB at 1.5 dpf, we later found that the following axons of ciliated OSNs from the same placode also failed to grow out (Fig. 9G,H; left side) and eventually accumulated at the border between the OE and the telencephalon by 3.5 dpf (arrowheads in Fig. 9H). By contrast, if a substantial number of the pioneer axons reached the presumptive OB by 1.5 dpf, we never detected impaired axon projection of ciliated OSNs at 3.5 dpf in *ody* mutant embryos (Fig. 9F-H; right side). In *ody/+* (Fig. 9A-D) and wild-type (data not shown) embryos, the pioneer axons always successfully navigated to the presumptive OB, and ciliated OSNs also established correct projection to the OB.

These results suggest that Cxcr4b-mediated signaling is important for pathfinding of zns-2-positive pioneer axons from unipolar neurons to exit the olfactory placode and that impaired pathfinding of the pioneer axons might be the reason why OSN axons subsequently fail to project to the OB in the absence of Cxcr4b function.

A permissive role for Cxcl12a in olfactory axon projection

The restricted expression of Cxcl12a along the path of olfactory axon navigation suggests that Cxcl12a might guide growing olfactory axons to the OB. To examine whether Cxcl12a plays a role as an attractive cue or a permissive substrate for olfactory axons, we heat shocked hsp:cxcl12a;omp:yfp double-transgenic embryos at 12 and 19 hpf, just before the olfactory placode assembly and just before the emergence of pioneer axons, respectively, and analyzed axon projection at 3.5 dpf. As described above, we found that ubiquitous expression of Cxcl12a at 12, but not 19, hpf perturbed the olfactory placode assembly (Fig. 5B,C). However, neither at 12 nor 19 hpf did ubiquitous expression of Cxcl12a induce significant defects in olfactory axon projection at 3.5 dpf (Fig. 5E,F). These results suggest that Cxcl12a does not guide olfactory axons as an attractive cue but rather creates a permissive environment for navigating olfactory axons. Importantly, these results also

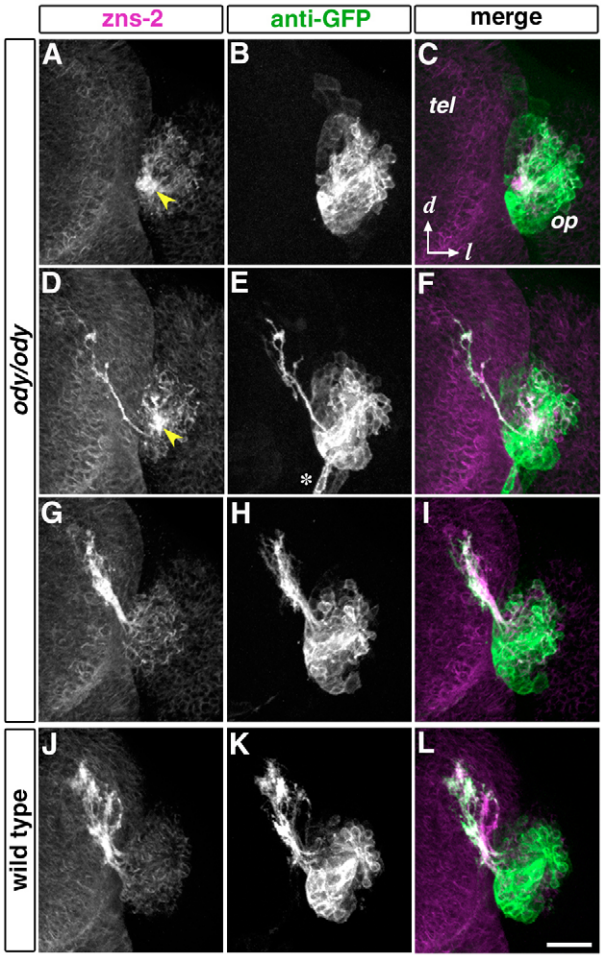

Fig. 8. Projection of pioneer axons is impaired in zebrafish *ody* mutant embryos. *ody/ody;omp:yfp/+* (**A-I**) and *omp:yfp/+* (**J-L**) embryos double labeled with zns-2 antibody (A,D,G,J; magenta in C,F,I,L) and anti-GFP antibody (B,E,H,K; green in C,F,I,L) at 1.5 dpf are shown in frontal views as *z*-stacked images. Projection patterns of pioneer axons in *ody* mutants vary, ranging from no axon reaching the presumptive OB (A-C) to an essentially normal projection (G-I). Note that projection defects with intermediate severity are observed (D-F). Arrowheads indicate accumulated zns-2-positive axons near the placode-telencephalon border. Scale bar: 50 μm. *d*, dorsal; *l*, lateral; *op*, olfactory placode; *tel*, telencephalon. The asterisk in E marks mispositioned olfactory neurons.

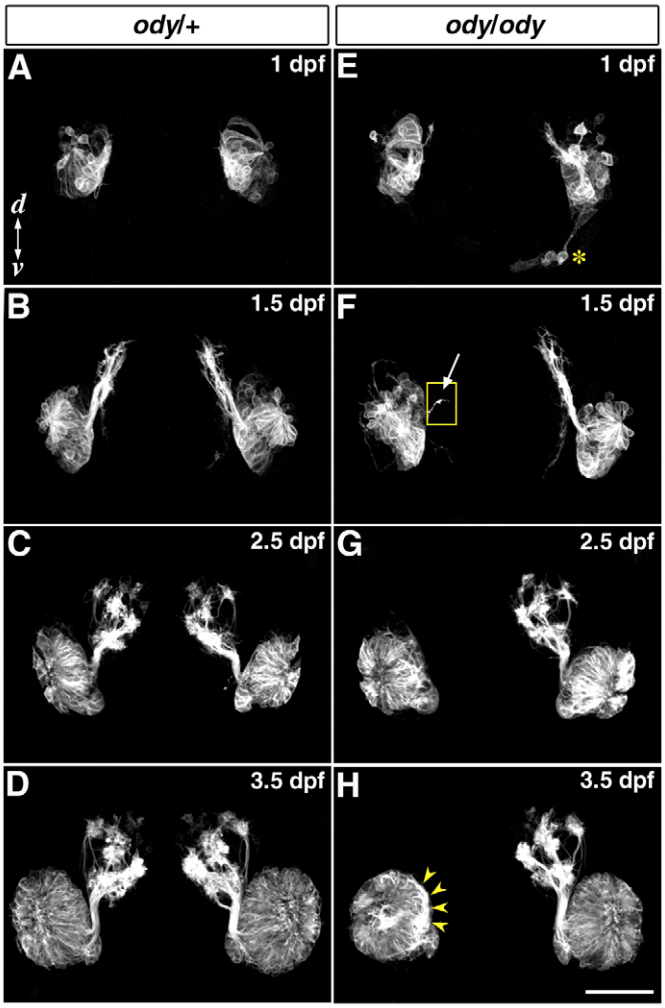

Fig. 9. Live imaging of axon projection in zebrafish *ody* mutant embryos. Developmental processes of axon projection in representative *ody/+;omp:yfp/+* (**A-D**) and *ody/ody;omp:yfp/+* (**E-H**) embryos are shown in frontal views. Yellow-boxed inset in F is shown at high gain to reveal faint axonal fibers. In the *ody/ody* embryo, pioneer axons extending toward the presumptive OB (arrow in F) from one of two olfactory placodes are significantly reduced in number at 1.5 dpf, when compared with those from the contralateral placode and *ody/+* placodes. When pathfinding by the pioneer axons is significantly impaired at 1.5 dpf, following OSN axons fail to exit the olfactory placode and eventually accumulate within the OE at 3.5 dpf (yellow arrowheads in H). The asterisk in E marks mispositioned olfactory neurons in the *ody/ody* embryo. Scale bar: 100 μm. *d*, dorsal; *v*, ventral.

demonstrate that axon guidance defects in the absence of Cxcr4b-mediated chemokine signaling cannot be attributed solely to the mispositioning of olfactory neuron cell bodies.

DISCUSSION

Olfactory placode assembly and subsequent OSN axon projection are two crucial aspects in the formation of functional neural circuitry of the primary olfactory system. Here, we found that these events depend on Cxcl12a chemokine signaling through its receptor Cxcr4b in zebrafish. Both loss and gain of function for the Cxcl12a/Cxcr4b signaling perturbed placode assembly of olfactory neuron precursors into a compact cluster. Furthermore, loss of function frequently resulted in a defect in pathfinding of pioneer axons, leading to a complete loss of OSN axon projection to the OB. These findings reveal a dual role of chemokine signaling in controlling cell migration and axon pathfinding in the zebrafish olfactory system.

Role of Cxcl12a/Cxcr4b signaling in olfactory placode assembly

Olfactory neuron precursors initially lie in the olfactory placodal field, the region stretching along the lateral edge of the anterior neural plate (Whitlock and Westerfield, 2000; Whitlock, 2004). As development progresses, they converge to form the olfactory placode. The region expressing *cxcr4b* in the anterior head corresponds to the olfactory placodal field. Previous studies have demonstrated that Cxcr4b-mediated signaling guides migration of various types of cells in different ways in zebrafish, including primordial germ cells (Doitsidou et al., 2002; Knaut et al., 2003), posterior lateral line primordia (David et al., 2002) and trigeminal sensory neurons (Knaut et al., 2005). The *cxcr4b*-expressing germ cells and posterior lateral line primordia move along their migratory route, maintaining direct contacts with the *cxcl12a* expression domains. By contrast, most *cxcr4b*-expressing trigeminal sensory neurons are initially located at a distance from the *cxcl12a* expression domains, and then move toward the Cxcl12a sources. These observations suggest that Cxcl12/Cxcr4 signaling may act in either short or long range, depending on the situations of individual cell types. In the case of olfactory neuron precursors, they are closely adjacent to the *cxcl12a* expression domain until the olfactory placode is formed, suggesting a short-range action of Cxcl12a in this process.

In the absence of Cxcr4b-mediated signaling, olfactory neuron precursors dispersed anteriorly, resulting in ventrally displaced olfactory neurons. Hence, chemokine signaling is required for correct positioning of olfactory neurons. Moreover, global and localized misexpression of Cxcl12a perturbed olfactory placode assembly, suggesting that Cxcl12a/Cxcr4b signaling is not merely permissive, but acts as a guidance cue to position the olfactory neurons. This notion is consistent with the observation that spatial restriction of the *cxcl12a* expression domain occurs synchronously with convergence of the olfactory placodal field. There is a significant anterior tissue movement during early segmental stages (Karlstrom and Kane, 1996), and this movement should result in ventral cell streaming at the most anterior part of the developing head. The appearance of ventrally displaced olfactory neurons in the absence of Cxcr4b signaling raises the possibility that Cxcl12a provides olfactory neuron precursors with a retention signal to withstand the anterior/ventral movement of neighboring cells. Our observation that ectopic Cxcl12a sources in the ventral region, but not in the dorsal region, can recruit olfactory neurons to positions close to the ectopic Cxcl12a sources could also be explained by the competition between the endogenous Cxcl12a source and the anterior/ventral streaming of cells expressing exogenous Cxcl12a. Such a mechanism, by which Cxcl12 might act to retain *cxcr4b*-expressing cells in the correct position, has been implicated in trigeminal sensory ganglion assembly (Knaut et al., 2005). In this case, *cxcl12* expression domains are located posteriorly adjacent to the final position of ganglia, opposite to the direction of morphogenetic movements. By contrast, the *cxcl12a* expression domain in the anterior head was positioned medially to the array of olfactory neuron precursors, although a similar mispositioning phenotype was observed in both olfactory neurons and trigeminal sensory neurons upon disruption of Cxcr4b signaling. Direct in vivo observations on dynamic behaviors of olfactory neuron precursors and neighboring cells in wild-type and *ody* mutant embryos may clarify the mode of Cxcl12a action in more detail.

Role of Cxcl12a/Cxcr4b signaling in olfactory axon pathfinding

In *ody* mutants, ~50% of the embryos exhibited defects in OSN axon projection to the OB. The simplest interpretation is that Cxcl12a may act as a chemoattractant for olfactory axons, because *cxcl12a* is expressed in the placode-telencephalon border where the axons cross to enter the telencephalon and also in the anterior tip of the telencephalon toward which the axons grow. However, Cxcl12 does not appear to exhibit obvious attractive activity when assayed on several classes of vertebrate neurons in vitro (Chalasani et al., 2003). Secondly, axon guidance defects might be an indirect consequence of loss of Cxcr4b signaling. In the absence of Cxcr4b signaling, olfactory neurons are mispositioned and outgrowing axons are challenged with a new micro-environment, and failure to interpret this new environment correctly may cause axons to navigate to new targets. However, such an indirect effect of loss of Cxcr4b signaling on axon guidance is unlikely, because ubiquitous misexpression of Cxcl12a at 12 hpf, which induces mispositioning of olfactory neurons, did not cause the *ody*-like OSN axon pathfinding defects (Fig. 5B,E). As Cxcl12 has been shown to reduce the growth cone responsiveness to chemorepellents in vitro (Chalasani et al., 2003) and in vivo (Chalasani et al., 2007), the third possibility is that exposure of olfactory axons to Cxcl12a at the placode-telencephalon border might reduce the growth cone responsiveness to chemorepellent factors that exist around the path of olfactory axon navigation, allowing them to exit the olfactory placode and to grow toward the OB. This permissive model is consistent with our observation that forced ubiquitous expression of Cxcl12a at either 12 or 19 hpf induces no significant defect in OSN axon projection to the OB (Fig. 5). A previous study (Yoshida et al., 2002) has demonstrated that alteration of protein kinase A (PKA) activity in olfactory axons is important for pathfinding and has proposed that the interaction of growing axons with the placode-telencephalon border may downregulate PKA signaling, modulating the response of growth cone to guidance cues. Cxcl12a hence appears to be a promising candidate to fulfill this function via Cxcr4b, which signals through Gi proteins, thereby decreasing the intracellular cyclic AMP level (Tran and Miller, 2003).

The defects in OSN axon projection in *ody* mutants are variable and appear to occur in an all-or-none manner. Once OSN axons can reach the OB, the pattern of proto-glomerular targeting by OSNs in *ody* mutants is indistinguishable from that in wild type. This all-or-none phenotype could be explained by the notion that pioneer axons provide a scaffold essential for subsequently projecting OSN axons (Whitlock and Westerfield, 1998; Miyasaka et al., 2005). Indeed, the pathfinding by pioneer axons was frequently impaired in *ody*

mutants. In some cases, a portion of zns-2-positive pioneer axons failed to exit the olfactory placode, but the remaining ones from the same placode could reach the OB at 1.5 dpf. Such defects with an intermediate severity are rarely observed in OSN axon projection at 3.5 dpf. These findings imply that there might be a threshold in the number of OB-reaching pioneer axons that is required for establishment of a sound projection of OSN axons. Our observation that mature OSNs did not express *cxcr4b* also suggests that Cxcr4b-mediated signaling influences the early growing axons from either unipolar neurons or newly differentiated immature OSNs.

Cxcl12/Cxcr4 signaling has recently been shown to regulate retinal axon projection in zebrafish (Li et al., 2005) and motor axon projection in mouse (Lieberam et al., 2005). In *cxcr4b* mutant zebrafish, some ganglion cell axons fail to exit the eye but extend in aberrant directions within the retina. Similarly, in the absence of Cxcr4 signaling in mice, some axons of a set of motoneurons, termed vMNs, aberrantly exit through the dorsal exit point of the spinal cord instead of correctly choosing the ventral exit point. In both cases, the initial phase of axon pathfinding is perturbed similarly to the case for olfactory axons deprived of Cxcr4b function. These findings suggest that Cxcl12/Cxcr4 signaling might be used as a general molecular tool to create a favorable environment and to shape an initial trajectory for various types of early growing axons in vertebrates.

We thank members of the Yoshihara laboratory for fish care and discussion, Nobuaki Tamamaki (Kumamoto University) for rabbit ant-GFP antibody and John Y. Kuwada (University of Michigan) for pHSP70/4-EGFP plasmid. H.K. thanks Alexander F. Schier (Harvard University) for support. This work was supported in part by a Grant-in-Aid for Scientific Research (B) to Y.Y. from the Ministry of Education, Culture, Sports, Science, and Technology of Japan. H.K. was supported by a long-term fellowship from the Human Frontier Science Program (HFSP). The transgenic fish line, Tg(OMP^{2k}:gap-YFP)^{rw032a}, can be obtained upon request under the support of Zebrafish National Bioresource Project of Japan.

Supplementary material

Supplementary material for this article is available at http://dev.biologists.org/cgi/content/full/134/13/2459/DC1

References

Bagri, A., Gurney, T., He, X., Zou, Y. R., Littman, D. R., Tessier-Lavigne, M. and Pleasure, S. J. (2002). The chemokine SDF1 regulates migration of dentate granule cells. *Development* **129**, 4249-4260.

Balabanian, K., Lagane, B., Infantino, S., Chow, K. Y., Harriague, J., Moepps, B., Arenzana-Seisdedos, F., Thelen, M. and Bachelerie, F. (2005). The chemokine SDF-1/CXCL12 binds to and signals through the orphan receptor RDC1 in T lymphocytes. *J. Biol. Chem.* **280**, 35760-35766.

Belmadani, A., Tran, P. B., Ren, D., Assimacopoulos, S., Grove, E. A. and Miller, R. J. (2005). The chemokine stromal cell-derived factor-1 regulates the migration of sensory neuron progenitors. *J. Neurosci.* **25**, 3995-4003.

Borrell, V. and Marin, O. (2006). Meninges control tangential migration of hem-derived Cajal-Retzius cells via CXCL12/CXCR4 signaling. *Nat. Neurosci.* **9**, 1284-1293.

Burns, J. M., Summers, B. C., Wang, Y., Melikian, A., Berahovich, R., Miao, Z., Penfold, M. E., Sunshine, M. J., Littman, D. R., Kuo, C. J. et al. (2006). A novel chemokine receptor for SDF-1 and I-TAC involved in cell survival, cell adhesion, and tumor development. *J. Exp. Med.* **203**, 2201-2213.

Chalasani, S. H., Sabelko, K. A., Sunshine, M. J., Littman, D. R. and Raper, J. A. (2003). A chemokine, SDF-1, reduces the effectiveness of multiple axonal repellents and is required for normal axon pathfinding. *J. Neurosci.* **23**, 1360-1371.

Chalasani, S. H., Sabol, A., Xu, H., Gyda, M. A., Rasband, K., Granato, M., Chien, C. B. and Raper, J. A. (2007). Stromal cell-derived factor-1 antagonizes slit/robo signaling in vivo. *J. Neurosci.* **27**, 973-980.

Chong, S. W., Emelyanov, A., Gong, Z. and Korzh, V. (2001). Expression pattern of two zebrafish genes, cxcr4a and cxcr4b. *Mech. Dev.* **109**, 347-354.

David, N. B., Sapède, D., Saint-Etienne, L., Thisse, C., Thisse, B., Dambly-Chaudière, C., Rosa, F. M. and Ghysen, A. (2002). Molecular basis of cell migration in the fish lateral line: role of the chemokine receptor CXCR4 and of its ligand, SDF1. *Proc. Natl. Acad. Sci. USA* **99**, 16297-16302.

de Castro, F. (2003). Chemotropic molecules: guides for axonal pathfinding and cell migration during CNS development. *News Physiol. Sci.* **18**, 130-136.

Doitsidou, M., Reichman-Fried, M., Stebler, J., Köprunner, M., Dörries, J., Meyer, D., Esguerra, C. V., Leung, T. and Raz, E. (2002). Guidance of primordial germ cell migration by the chemokine SDF-1. *Cell* **111**, 647-659.

Elsalini, O. A. and Rohr, K. B. (2003). Phenylthiourea disrupts thyroid function in developing zebrafish. *Dev. Genes Evol.* **212**, 593-598.

Guan, K. L. and Rao, Y. (2003). Signaling mechanisms mediating neuronal responses to guidance cues. *Nat. Rev. Neurosci.* **4**, 941-956.

Halloran, M. C., Sato-Maeda, M., Warren, J. T., Su, F., Lele, Z., Krone, P. H., Kuwada, J. Y. and Shoji, W. (2000). Laser-induced gene expression in specific cells of transgenic zebrafish. *Development* **127**, 1953-1960.

Karlstrom, R. O. and Kane, D. A. (1996). A flipbook of zebrafish embryogenesis. *Development* **123**, 461.

Kimmel, C. B., Ballard, W. W., Kimmel, S. R., Ullmann, B. and Schilling, T. F. (1995). Stages of embryonic development of the zebrafish. *Dev. Dyn.* **203**, 253-310.

Knaut, H., Pelegri, F., Bohmann, K., Schwarz, H. and Nüsslein-Volhard, C. (2000). Zebrafish vasa RNA but not its protein is a component of the germ plasm and segregates asymmetrically before germline specification. *J. Cell Biol.* **149**, 875-888.

Knaut, H., Werz, C., Geisler, R. and Nüsslein-Volhard, C. (2003). A zebrafish homologue of the chemokine receptor Cxcr4 is a germ-cell guidance receptor. *Nature* **421**, 279-282.

Knaut, H., Blader, P., Strähle, U. and Schier, A. F. (2005). Assembly of trigeminal sensory ganglia by chemokine signaling. *Neuron* **47**, 653-666.

Li, Q., Shirabe, K., Thisse, C., Thisse, B., Okamoto, H., Masai, I. and Kuwada, J. Y. (2005). Chemokine signaling guides axons within the retina in zebrafish. *J. Neurosci.* **25**, 1711-1717.

Lieberam, I., Agalliu, D., Nagasawa, T., Ericson, J. and Jessell, T. M. (2005). A Cxcl12-Cxcr4 chemokine signaling pathway defines the initial trajectory of mammalian motor axons. *Neuron* **47**, 667-679.

Miyasaka, N., Sato, Y., Yeo, S. Y., Hutson, L. D., Chien, C. B., Okamoto, H. and Yoshihara, Y. (2005). Robo2 is required for establishment of a precise glomerular map in the zebrafish olfactory system. *Development* **132**, 1283-1293.

Mizuno, T., Kawasaki, M., Nakahira, M., Kagamiyama, H., Kikuchi, Y., Okamoto, H., Mori, K. and Yoshihara, Y. (2001). Molecular diversity in zebrafish NCAM family: three members with different VASE usage and distinct localization. *Mol. Cell. Neurosci.* **18**, 119-130.

Sato, Y., Miyasaka, N. and Yoshihara, Y. (2005). Mutually exclusive glomerular innervation by two distinct types of olfactory sensory neurons revealed in transgenic zebrafish. *J. Neurosci.* **25**, 889-897.

Schwarting, G. A., Henion, T. R., Nugent, J. D., Caplan, B. and Tobet, S. (2006). Stromal cell-derived factor-1 (chemokine C-X-C motif ligand 12) and chemokine C-X-C motif receptor 4 are required for migration of gonadotropin-releasing hormone neurons to the forebrain. *J. Neurosci.* **26**, 6834-6840.

Stumm, R. K., Zhou, C., Ara, T., Lazarini, F., Dubois-Dalcq, M., Nagasawa, T., Höllt, V. and Schulz, S. (2003). CXCR4 regulates interneuron migration in the developing neocortex. *J. Neurosci.* **23**, 5123-5130.

Tissir, F., Wang, C. E. and Goffinet, A. M. (2004). Expression of the chemokine receptor Cxcr4 mRNA during mouse brain development. *Brain Res. Dev. Brain Res.* **149**, 63-71.

Tran, P. B. and Miller, R. J. (2003). Chemokine receptors: signposts to brain development and disease. *Nat. Rev. Neurosci.* **4**, 444-455.

Westerfield, M. (1995). *The Zebrafish Book*. Eugene, OR: University of Oregon Press.

Whitlock, K. E. (2004). A new model for olfactory placode development. *Brain Behav. Evol.* **64**, 126-140.

Whitlock, K. E. and Westerfield, M. (1998). A transient population of neurons pioneers the olfactory pathway in the zebrafish. *J. Neurosci.* **18**, 8919-8927.

Whitlock, K. E. and Westerfield, M. (2000). The olfactory placodes of the zebrafish form by convergence of cellular fields at the edge of the neural plate. *Development* **127**, 3645-3653.

Xiang, Y., Li, Y., Zhang, Z., Cui, K., Wang, S., Yuan, X. B., Wu, C. P., Poo, M. M. and Duan, S. (2002). Nerve growth cone guidance mediated by G protein-coupled receptors. *Nat. Neurosci.* **5**, 843-848.

Yoshida, T., Ito, A., Matsuda, N. and Mishina, M. (2002). Regulation by protein kinase A switching of axonal pathfinding of zebrafish olfactory sensory neurons through the olfactory placode-olfactory bulb boundary. *J. Neurosci.* **22**, 4964-4972.

Zhu, Y., Yu, T., Zhang, X. C., Nagasawa, T., Wu, J. Y. and Rao, Y. (2002). Role of the chemokine SDF-1 as the meningeal attractant for embryonic cerebellar neurons. *Nat. Neurosci.* **5**, 719-720.